Pre-assessment of the Potential Dual Polarization Sentinel-1 Data for Mapping the Mangrove Tree Species Distribution in South Bali, Indonesia

1st Mochamad Firman Ghazali
Department of Geodesy and Geomatics Engineering,
Faculty of Engineering, University Lampung
Bandar Lampung, Indonesia
firman.ghazali@eng.unila.ac.id

2nd Ketut WIkantika
Department of Geodesy and Geomatics Engineering,
Faculty of Earth Sciences and Technology, ITB
Bandung, Indonesia
wikantika.ketut@gmail.com

Abstract— Behind the needs of the availability for the mangrove trees biodiversity database are important in promoting coastal area protection, includes mangrove forest conservation. This initiative started by mapping mangrove trees distribution by utilizing two different modes of ground detected ranged (GRD) and single look complex (SLC) of Sentinel-1 data images. Both are processed to get the backscatter value, dual-polarization radar vegetation index (DpRVI) and polarization decomposition for entropy, alpha, and anisotropy values for each mangrove trees species (MTS) detection that compared with the data field. Besides that, the distribution of each mangrove tree has been conducted based on its genus and species richness that estimated using a random forest (RF) algorithm for nine different combinations, includes VV, VH, and VV-VH, entropy, alpha, and anisotropy, DpRVI, and the integration of between backscatter value and polarization decomposition. The result has shown a variation in the level of accuracy ranged from weak to moderate at about 26% to 65%. The combination of VV, VH, VH-VV and DpRVI obtained better accuracy at about 65%. Related to the species of mangrove detected, the Avicennia alba becomes a dominant mangrove tree species grown as much as 60% in the study area.

Keywords: Mangrove trees, coastal conservation, random forest, Sentinel-1

I. INTRODUCTION

Historically, various remote sensing data are often used as the primary input for biodiversity assessment. In vegetation studies, a very long journey of radar data focuses on vegetation studies are very challenging [1]. Last two decades, Simard et al. [2] studied the basic function of combination ERS-1 and JERS-1 Synthetic Aperture Radar (SAR) in mapping tropical coastal vegetation using a decision tree classifier. This combination of two different bands of L and C-band, and polarization type of VV and HH, respectively are useful for woody vegetation distinguish from other types of vegetation. Even though this work has only detected the major types of coastal vegetation, and similar to the land cover type such as grass and woody savanna, flooded vegetation and also mangroves, in general. Precisely, some studies showed better results but need additional data such as optical imagery like Landsat imageries. Sano, Ferreira and Huete, [3] have proven the capabilities of this integration method, but the limitation shows the use of vegetation indices derived from the optical data is still the best. Considering the combination of two different types of remote sensing data is still promising.

Deriving tree species richness from several types of radar images are important. It takes to the basic knowledge of biodiversity status and the needs of promoting conservation. Both backscatter, interferometry and polarization characteristic have their potential in understanding the vegetation structures. Furthermore, the study conducted by Simard [4] has successfully made a critical review on how those radar parameters are useful to gain some of the major information of mangroves. It is supported by Proisy et al and Lucas et al [5], [6], both types of research have found the benefits of utilizing radar images especially in differentiate the mangrove trees. Divided into two major groups, includes shrub and tall mangroves. This vegetation can be found at -20 to -15dB and -14dB for shrub and tall mangroves in the C band with HV polarization, respectively. For the C band with VV polarization, both types of mangroves were found at about -12dB and-6dB.

Those bands with similar polarization are owned by the Sentinel 1 satellite image that was produced by two identical satellites Launched on 3rd April 2014 and 25th April 2016. It was an imaging radar system with 12 days repeat cycle and 20 meters spatial resolution. Offering high resolution, it was promising to map land cover [7] winter crop pattern using backscattering coefficient (σ^0). Denize et al.[8] developed the first dual polarimetric radar vegetation index (DpRVI), it can be used for crop monitoring and complementary data for optical image results in the analysis [9], [10]. For mangrove observation based on Sentinel 1 data, several studies have been conducted to map the distribution of above-ground biomass (AGB) [11], differentiate mangroves and non-mangroves based on texture and segmentation analysis [12], and a decision trees application for mangroves species detection and mapping [13], but still required the optical images of Sentinel 2.

The use of the polarization decomposition technique offering optimised results. It developed previously in quad polarization data, such as Alos Palsar. One of the studies that reported a promising result in distinguishing the mangrove species is conducted by Brown et al. [14]. Four mangroves species were identified. For the dual-polarization data like Sentinel 1, at least the studies conducted by Li and Bijker, Prudente et al., and Harfenmeister et al. [15]–[17] explained the potential for this type of handling of the SLC data product to observe the vegetation characteristics and its biophysical parameters.

For that reason, it might be possible to study the mangrove species distribution using Sentinel-1 data. This research aimed to maximize the dual-polarization of Sentinel 1 for differentiating tree mangroves species. Both GRD and

SLC data formats of Sentinel 1 that are processed to derive backscatter values, polarization decomposition, and dual-polarization radar vegetation index (DpRVI) must be used for calculating a random forest algorithm. The validation itself will employ the species richness from the fieldwork.

II. METHODOLOGY

A. Study location

The study of mangrove trees species observation has taken place in the Mangrove Forest Management Center in Bali, Indonesia (Figure 1). At this place are growing more than 60 species of mangroves, include primary or true and minor or secondary groups of mangroves [18]. The mangroves forest itself are located near the Bali Mandala toll road and the Tanjung Benoa bay and administratively located in the Pemogan village, South Denpasar District, the city of Denpasar (Figure 1). While the total mangrove forest covered an area of about 1136.66 hectares and was divided into several subdistricts.

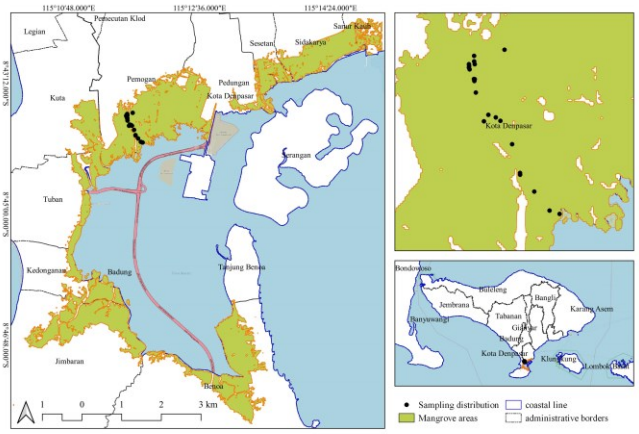

Figure 1 Study location of Mangrove Forest Management Center in Bali, Indonesia

B. Data

Two different types of radar data used include a level-1 of dual-polarization Sentinel 1 in the ground range detected (GRD) and single look complex (SLC) data format is used for mapping the mangrove tree species distribution in South Bali, Indonesia. Both data were obtained from The Alaska satellite facility at no cost. Details of SAR data used to map mangrove is provided in the table below (Table 1).

Table 1 Data used for observing the mangrove trees in the Bali Mangrove Forest Management Center

No	Type	Mode	Swath Mode	Acquisition time	Polarization
1	S1	SLC	IW	2020/11/13	VV+VH
2	S1	GRD	IW	2020/11/13	VV+VH

Fieldwork has been conducted in the Mangrove Forest Management Center to collected geo-located mangrove trees species and successfully identified as many as 9 species, and 23 point samples that consist of *Aegiceras corniculatum, Avicennia marina, Avicennia officinalis, Avicennia rumphiana, Excoecaria agallocha, Hibiscus tiliaceus, Rizhopora apiculata, Rhizophora mucronata*, and *Soneratia alba* from the total 60 species has successfully collected, while the identification process of mangrove trees species is based on the guidance provided in Noor and Khazali, [18], [19]. From the total collected samples, was divided into two groups that consist of 9 and 14 selected samples were used for training samples on classification and ground truth stage, respectively.

C. Data processing

1. Sentinel-1 GRD data pre-processing

The Sentinel-1 data were pre-processed using the Sentinel application platform (SNAP). The processing steps included apply orbit, radiometric calibration to the sigma 0 values, speckle filtering using 3*3 of Lee sigma algorithm to minimize salt and pepper in the Sentinel-1 image [20], [21], range-doppler terrain correction using SRTM digital elevation model, and conversion from linear to decibel scale.

2. Mangroves areas delineation

The corrected Sentinel-1 data images were used to delineate the mangroves areas. This step is necessary to keep the machine is running well, due to a limitation of memory by decrease the data size. The entire mangrove area has been delineated using the method suggested by Dostálová et al. [22].

3. Mangrove trees backscatter values estimation for GRD data

The masked of corrected Sentinel-1 is defined as the mangrove area. Then, It should have corresponded with the observed mangrove trees species collected from the field. Each pixel that corresponds to the location of the observed mangrove trees had extracted and considered as the mangrove back-scatter values. Each mangrove species is expected to have different values, so they can be distinguished from each other.

4. Decomposition of polarization values estimation for SLC data

The decomposition polarization, includes entropy, alpha, and anisotropy derived from a single look complex (SLC). It requires phase information instead of intensity on each VV and VH polarization. The mangrove forest varies in canopy density, and plant height. Both biophysical parameters can influence the backscatter mechanism that occurs in the mangrove areas, which dominate by a volume scattering [23]. It is similar to the rain forest in general or other dense vegetation covers [24]. Distinguishing the mangrove trees species through their volume scattering characteristics are valuable to differentiate the species distribution. All three parameters are derived using the SNAP that involved the following steps, such as apply orbit, slice assembly, topsar-split, topsar-deburst, topsar merge, polarimetric matrices, multi look, polarimetric speckle filtering, polarimetric decomposition, and terrain correction.

5. Biophysical parameters estimation through the estimation dual-polarization radar vegetation index (DpRVI)

The modified Radar Vegetation Index (RVI) namely dual-polarization radar vegetation index (DpRVI) developed by Mandal et al [10] (Eq.1). While the RVI itself was developed by Kim and Van Zyl [25], but it is used only for Quad-polarization data like Radarsat (Eq.2). It's expected As

plant canopy advances from early leaf development to the fully vegetative stage, the DpRVI increases from 0 to 1[10].

$$DpRVI=((4*\sigma VH))/((\sigma VV+\sigma VH)) \quad (1)$$

$$RVI=((8*\sigma HV))/((\sigma HH+\sigma VV+2\sigma HV)) \quad (2)$$

6. Supervised classification using random forest algorithm

The use of random forest classification in observing the forest has been introduced by Liu et al. [26]. It used several combinations of satellite data and given better accuracy than only used only a single data set. In this study, the same technique was applied using several different configurations, but only utilize the synthetic aperture radar data of Sentinel-1 in GRD for the combination of VV, VH, and VV/VH or VV-VH, three parameters of decomposition polarimetric and dual-polarization radar vegetation index (DpRVI) (Tabel 2).

Table 2 Configuration for mangroves trees classification using the Random Forest Algorithm

No	Data Combination
1	VV
2	VH
3	VV, VH, VH-VV
4	VV, VH, VH/VV
5	entropy, alpha, anisotropy
6	VV, VH, VH-VV, entropy, alpha, anisotropy
7	DpRVI
8	entropy, alpha, anisotropy, DpRVI
9	VV, VH, VH-VV, entropy, alpha, anisotropy, DpRVI

III. Result and Discussion

A. Backscatter values of mangroves tress

The mangroves area are similar to others forested area. It has the highest backscatter values especially in VH [22]. This area is prone to experience some disturbances, like deforestation by converting the forested area into a fish or shrimp pond. It makes the density of tree cover decrease and indicates low to medium backscatter values [27]. According to Proisy et al. [5], [6], the values of backscatter are influenced by the canopy structure. It will increase when the canopy is growing larger, as it can be found at -20 to -15dB and -14dB for shrub and tall mangroves in the C band with HV polarization, respectively. For the C band with VV polarization, both types of mangroves were found at about -12dB and-6dB. It is similar to Bouman [28], the backscatter values are increased when the size of vegetation is increase, especially in crops. In the study area, the mangrove trees are growing at about 2 – 15 meters of height. *Rhizophora mucronata* is the tallest mangrove tree found there.

The *Avicennia sp*. can be found at a range of 0.49 to 0.67 dB at VV/VH. It is equal with 4.33 to 7.66 dB in VV-VH, -7.11 to -9.04 dB in VV, and -12.75 to -15.15 dB in VH. For both cross-polarization, the backscatter values in VV are always higher than VH. Both are different responses in the area of volume scattering influence by mangrove trees canopy. Studies have shown the same behaviour as stated by Nicolau et al. [29]. This pattern is similar to two other species, includes *Rizhopora sp*. and *Soneratia sp*. Although, it was contrary to Dubois et al. [30] that the objects with volume scattering like forested areas tend to have a higher backscatter in VH. Details for all backscatter values of each mangrove tree extracted from the GRD data are available in Table 3.

Table 3 Backscatter values for Mangrove trees species

No	Mangrove Species	VV/VH		VV-VH		VV		VH	
		Min	Max	Min	Max	Min	Max	Min	Max
1	*Aegiceras corniculatum*	0.54929		6.16260		-7.51041		-13.67301	
2	*Avicennia marina*	0.49403	0.66476	4.49240	7.66930	-8.90804	-7.48830	-15.15759	-13.37401
3	*Avicennia officinalis*	0.57753	0.63673	4.76821	5.38722	-8.35776	-7.36449	-13.12598	-12.75171
4	*Avicennia rumphiana*	0.53979	0.67601	4.33652	6.06275	-9.04807	-7.11105	-13.38459	-13.17380
5	*E. agallocha*	0.62135		4.76197		-7.81413		-12.57610	
6	*H. tiliaceus*	0.64370		4.73515		-8.55458		-13.28973	
7	*Rizhopora apiculata*	0.61802	0.79510	2.73850	5.09625	-10.62658	-8.24558	-13.36508	-13.34183
8	*Rizhopora mucronata*	0.57061	0.62135	4.76197	5.67240	-8.03821	-7.46639	-13.71061	-12.57610
9	*Soneratia alba*	0.58627	0.70083	4.19102	5.53677	-10.62878	-7.50457	-15.23782	-12.80053

B. Polarization decomposition for mangroves tress detection

Have been reported previously by Mengmeng and Wijker [15], the use of polarization decomposition technique are useful for detection and classification the vegetable in the field. Another study was using the same technique, also given the similar result reported by Prudente et al. [16]. It must be the same result that can be obtained in this study. The *Aegicerassp., E. agallocha,* and *H. tiliaceus* are minority species of associate mangrove and tend to have a random distribution in a smaller group compared with other species. This situation influenced the values of anisotropy, entropy, and alpha of each species looks confusing. For instant, the ranges values of *Avicennia sp.* at about 0.518 to 0.538 is located between the values of *Aegiceras corniculatum* at 0.537and it applied to two other mangroves named *E. agallocha*, and *H. tiliaceus* and finally contribute to the classification processes in distinguishing each mangrove species (Table 4). The situation that occurred in anisotropy values is not the same with entropy and alpha. Each mangrove species observed in the field have different values. It can be assumed that the used both entropy and alpha are better in prediction and classification processes compared to anisotropy.

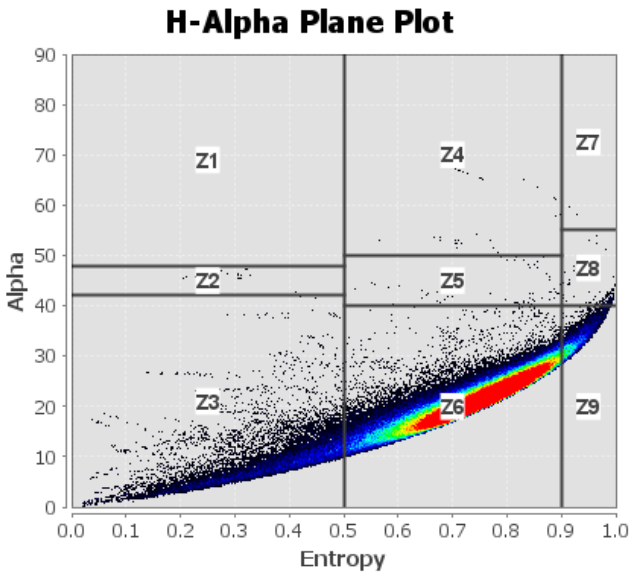

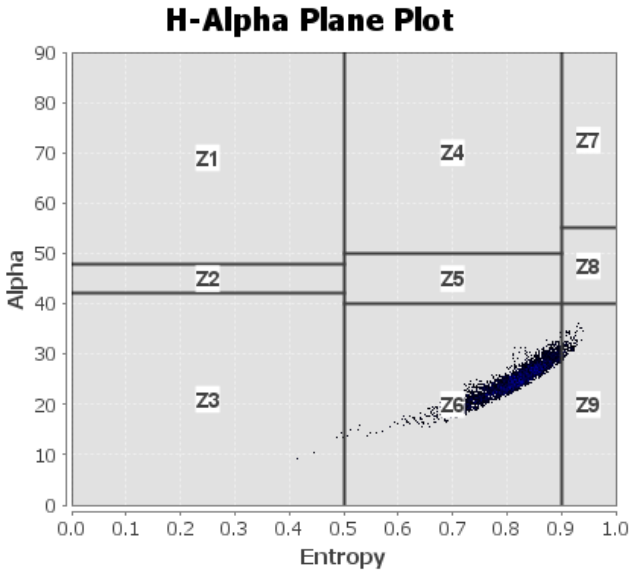

The combination between alpha and entropy values obtained from the decomposition polarization processes can be display as a H-alpha plot. This plot is divided the polarimetric values into nine zone describing the backscatter mechanism occur into the objects. For the entire mangrove area, the polarimetric values fall into the Z3, Z6, and Z9 which is represented a bragg surface, random surface, and non-feasible, respectively.

C. Mangrove dual-polarization radar vegetation index (DpRVI)

As well as the polarization decomposition, the DpRVI has also observed and got the values to range at about 0.567 to 0.657 that correspond with nine species of mangrove (Table 4). According to these values, it seems the DpRVI offered the better capability to use as parameter input for detection of the mangrove trees species. Mandal et al. [10] have proven the capability of DpRVI to assess the plant growth dynamics that have special characteristics at each stage. Physically, the plant growth associated with the canopy size, plant height, and biomass content, with this normal range of DpRVI values, might contribute well to the classification process as well as the entropy and alpha.

Table 4 decomposition polarization and DpRVI for Mangrove trees species

No	Mangrove Species	Anisotropy	Entropy	Alpha	DpRVI
1	*Aegiceras corniculatum*	0.537	0.779	23.198	0.582
2	*Avicenia marina*	0.553	0.763	23.284	0.567
3	*Avicenia officinalis*	0.518	0.795	23.453	0.612
4	*Avicenia rumphiana*	0.538	0.776	22.762	0.596
5	*E. agallocha*	0.543	0.774	21.962	0.600
6	*H. tiliaceus*	0.505	0.807	24.528	0.619
7	*Rizhopora apiculata*	0.477	0.828	25.401	0.657
8	*Rizhopora mucronata*	0.533	0.783	22.405	0.584
9	*Soneratia alba*	0.503	0.807	25.607	0.609

The RGB combination for the red channel as VV, green channel as VH, and VV-VH in the blue channel gave the entire mangrove forest area in bright to dark blue colour. The area with the dark blue colour may be represented the dense mangrove areas, while the bright blue colour for a less dense mangrove cover. It is similar to the RDB visualisation as the entropy, alpha and anisotropy combination in the red, green, and blue channels respectively. The high density of mangroves is displayed in dark blue. This area is cover dominantly by the mangrove from the genus of Rhizophora. As for the DpRVI, the area with green to the blue colour represented the same type of mangrove. By using these combinations, the specific information of each species is unable to define. It must be put into the sophisticated classification process, and the random forest algorithm was the choice in this study. The situation of backscatter values, polarization decomposition and DpRVI maps is shown in figure 2.

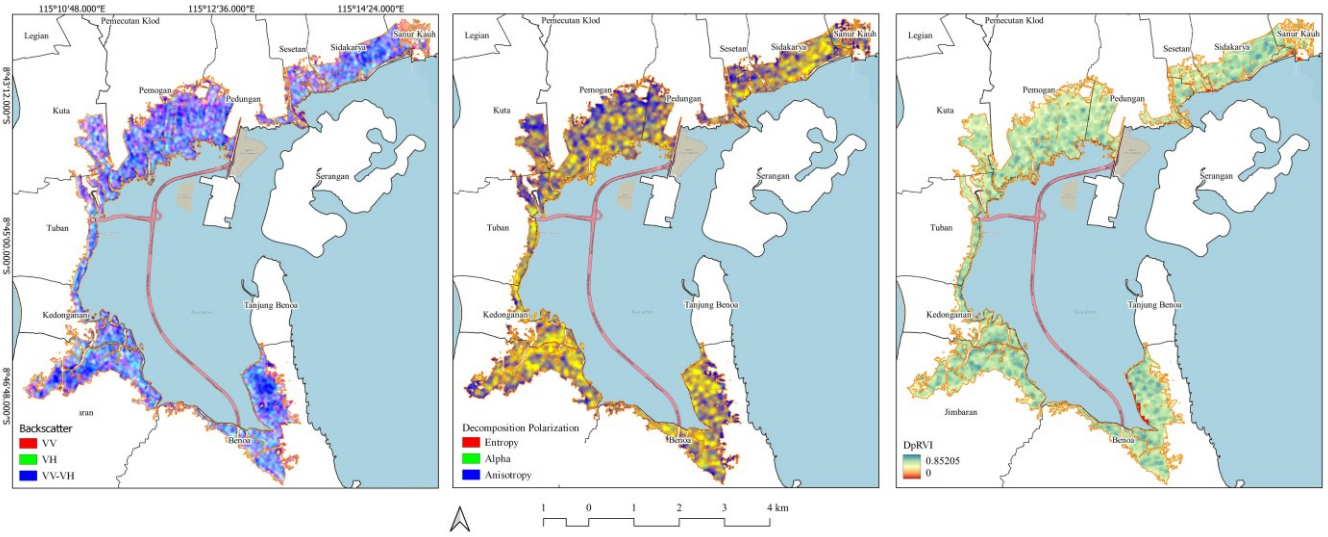

Figure 2 Processed Sentinel -1 data to backscatter, decomposition polarization and DpRVI

D. Comparison of random forest classification

There are nine combinations of backscatter, decomposition polarization, and DpRVI that are involved in the classification process using a random forest algorithm. As the result, there is also variation not only in the distribution of detected mangrove trees but also in the level of accuracy. In general, the use of single input for example just only use a VV, or DpRVI band are provided capability in detecting the same objects in the area compared with the three-band combination of an RGB like VV, VH, VV-VH; VV, VH, VH/VV, and the textural information from entropy, alpha, and anisotropy are expecting the promising result of the classification. Although, the combination between the backscatter values, textural characteristics, and the DpRVI that believe as the closest representation of vegetation characteristics should be more useful to solve the trees species mapping problems.

Table 5 comparison accuracy level of data combination used in classification Mangrove trees in genus and species level based on the random forest algorithm

No	Data Combination	Accuracy	
		Genus	Species
1	VV	39%	30%
2	VH	35%	26%
3	VV, VH, VH-VV	43%	43%
4	VV, VH, VH/VV	48%	43%
5	entropy, alpha, anisotropy	61%	39%
6	VV, VH, VH-VV, entropy, alpha, anisotropy	57%	57%
7	DpRVI	43%	30%
8	entropy, alpha, anisotropy, DpRVI	65%	48%
9	VV, VH, VH-VV, entropy, alpha, anisotropy, DpRVI	39%	26%

As shown in Table 5, those combinations of random forest classification input have a different level of accuracy and ability to put them into a range of level accuracy from the weak to the moderate. All the single inputs, consist of VV, VH, DpRVI are grouped as the weakest for both genus and species classification scenarios. It ranges from 35% to 43% and 26% to 36% for genus and species distribution, respectively. As the improvement has shown from the RGB combinations like VV, VH, VH-VV; VV, VH, VH/VV, and entropy, alpha, anisotropy. Especially in the genus scenario, the classification accuracy has increased from 48% to 61%, and 39% to 43% in the species scenario. At this stage, the consideration for using the RGB combination is better while it is used for detecting the mangrove trees based on their genus richness. For the trees species mapping, it is capable to rise the mapping quality even it is still lower compared to the performance of the same combination in trees genus mapping.

But, other results show that the combination of two RGB combinations consist of backscatter values from VV, VH, and VH-VV, and textural information obtained from the entropy, alpha, and anisotropy is better that increases as much as 7% accuracy compare to the single combination of RGB. Even though the combination of backscatter values from VV, VH, and VH-VV with vegetation characteristics represented by DpRVI has obtained the better result that

reached 65% accuracy. Overall, the scenarios used in the random forest algorithm to evaluate the capability of Sentinel 1 satellite data for both SLC and GRD are potential for mapping the mangrove trees distribution.

The opportunities come to improve the level of accuracy can be started by increasing the number of sampling points. And make sure that it distributes well in entire the location, even though it was a bit difficult because of the limitation of accessibility to enter the mangrove forest more deeply. To conserve the mangrove trees and their habitats. Besides that limitation, the map of mangrove trees distribution based on the better accuracy is reasonable if compare to the reality in the field. According to observation the genus of Avicennia sp. is the largest mangrove type grown in the Mangrove Forest Management Center in Bali (Figure 2).

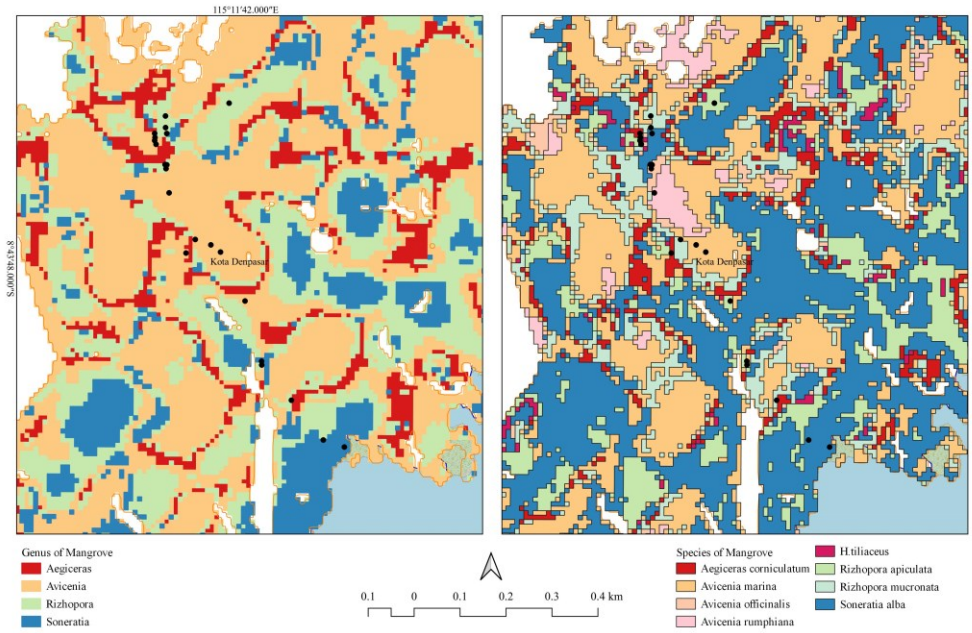

Figure 3 classification result of random forest algorithm for mangrove trees based on the best accuracy of genus and species richness

IV. Conclusion

Classifying the mangrove trees species are very challenging. The result ranges from lowest to moderate level of accuracy but not enough to declare it already was a good performance since this research is deal with several limitations, the sampling amount and its distribution was the critical point. But, it was promising if used for mapping the mangrove trees based on their genus. The use of radar data for classification is different from optical since many biophysical parameters are easily observed and represented by several indices. For further studies, it must be defined other dual-polarization formulas for observing the biophysical parameter and used together with DpRVI are possible to gain better accuracy and also better map mangrove trees distribution.

References

[1] J. B. de Jesus and T. M. Kuplich, "Applications of sar data to estimate forest biophysical variables in Brazil," Cerne, vol. 26, no. 1, pp. 88–97, 2020, doi: 10.1590/01047760202026012656.

[2] M. Simard, G. De Grandi, S. Saatchi, and P. Mayaux, "Mapping tropical coastal vegetation using JERS-1 and ERS-1 radar data with a decision tree classifier," Int. J. Remote Sens., vol. 23, no. 7, pp. 1461–1474, 2002, doi: 10.1080/01431160110092984.

[3] E. E. Sano, L. G. Ferreira, and A. R. Huete, "Synthetic aperture radar (L band) and optical vegetation indices for discriminating the Brazilian savanna physiognomies: A comparative analysis," Earth Interact., vol. 9, no. 15, 2005, doi: 10.1175/EI117.1.

[4] M. Simard, "Radar Remote Sensing of Mangrove Forests," SAR Handb. Compr. Methodol. For. Monit. Biomass Estim., p. 12, 2019, doi: 10.25966/33zm-x271.

[5] C. Proisy, E. Mougin, F. Fromard, V. Trichon, and M. A. Karam, "On the influence of canopy structure on the radar backscattering of mangrove forests," Int. J. Remote Sens., vol. 23, no. 20, pp. 4197–4210, 2002, doi: 10.1080/01431160110107725.

[6] R. M. Lucas, A. L. Mitchell, A. Rosenqvist, C. Proisy, A. Melius, and C. Ticehurst, "The potential of L-band SAR for quantifying mangrove characteristics and change: case studies from the tropics," Aquat. Conserv. Mar. Freshw. Ecosyst., vol. 17, pp. 245–264, 2007, doi: 10.1002/aqc.833.

[7] S. Abdikan, F. B. Sanli, M. Ustuner, S. A. Radar, and S. V. Machines, "Land cover mapping using Sentinel-1 SAR data," in The International Archives of the Photogrammetry, Remote Sensing and Spatial Information Sciences, 2016, vol. XLI, pp. 757–761, doi: 10.5194/isprsarchives-XLI-B7-757-2016.

[8] J. Denize, L. Hubert-Moy, J. Betbeder, S. Corgne, J. Baudry, and E. Pottier, "Evaluation of using sentinel-1 and -2 time-series to identifywinter land use in agricultural landscapes," Remote Sens., vol. 11, no. 1, 2019, doi: 10.3390/rs11010037.

[9] M. Fauvel et al., "Prediction of plant diversity in

grasslands using Sentinel-1 and -2 satellite image time series," Remote Sens. Environ., vol. 237, no. November 2019, p. 111536, 2020, doi: 10.1016/j.rse.2019.111536.

[10] D. Mandal et al., "Dual polarimetric radar vegetation index for crop growth monitoring using sentinel-1 SAR data," Remote Sens. Environ., vol. 247, no. January, p. 111954, 2020, doi: 10.1016/j.rse.2020.111954.

[11] R. Jay Labadisos Argamosa et al., "Modelling above ground biomass of mangrove forest using Sentinel-1 imagery," ISPRS Ann. Photogramm. Remote Sens. Spat. Inf. Sci., vol. 4, no. 3, pp. 13–20, 2018, doi: 10.5194/isprs-annals-IV-3-13-2018.

[12] M. Arief, N. Anggraini, S. W. Adawiah, M. Hartuti, and N. Suwargana, "Aplikasi Data Satelit Radar Sentinel-1A Guna Deteksi Hutan Mangrove Studi Kasus : Segara Anakan , Kabupaten Cilacap," in Seminar Nasional Penginderaan Jauh ke-4 Tahun 2017, 2017, pp. 277–289.

[13] T. D. Pham, J. Xia, G. Baier, N. N. Le, and N. Yokoya, "Mangrove Species Mapping Using Sentinel-1 and Sentinel-2 Data in North Vietnam," in International Geoscience and Remote Sensing Symposium (IGARSS), 2019, pp. 6102–6105, doi: 10.1109/IGARSS.2019.8898987.

[14] I. Brown, S. Mwansasu, and L. O. Westerberg, "L-band polarimetric target decomposition of mangroves of the rufiji delta, Tanzania," Remote Sens., vol. 8, no. 2, 2016, doi: 10.3390/rs8020140.

[15] M. Li and W. Bijker, "Potential of multi-temporal sentinel-1A dual polarization SAR images for vegetable classification in Indonesia," in International Geoscience and Remote Sensing Symposium (IGARSS), 2018, pp. 3820–3823, doi: 10.1109/IGARSS.2018.8517325.

[16] V. H. R. Prudente, L. V. Oldoni, D. C. Vieira, C. E. V. Cattani, and I. Del'Arco Sanches, "Relationship between SAR/Sentinel-1 polarimetric and interferometric data with biophysical parameters of agricultural crops," Int. Arch. Photogramm. Remote Sens. Spat. Inf. Sci. - ISPRS Arch., vol. 42, no. 3/W6, pp. 599–607, 2019, doi: 10.5194/isprs-archives-XLII-3-W6-599-2019.

[17] K. Harfenmeister, S. Itzerott, C. Weltzien, and D. Spengler, "Agricultural monitoring using polarimetric decomposition parameters of sentinel-1 data," Remote Sens., vol. 13, no. 4, pp. 1–28, 2021, doi: 10.3390/rs13040575.

[18] Y. R. Noor, M. Khazali, and I. N. N. Suryadiputra, Panduan Pengenalan Mangrove di Indonesia, 2nd ed. Bogor: Wetlands International-Indonesia Programme, 2006.

[19] I. N. N. S. Rusila Noor, Y., M. Khazali, Pengenalan Mangrove di Indonesia. Bogor: PHKA-Wetlands International-Indonesia Programme, 1999.

[20] S. Medasani and G. U. Reddy, "Analysis and Evaluation of Speckle Filters by Using Polarimetric Synthetic Aperture Radar Data Through Local Statistics," Proc. 2nd Int. Conf. Electron. Commun. Aerosp. Technol. ICECA 2018, no. March, pp. 169–174, 2018, doi: 10.1109/ICECA.2018.8474567.

[21] J. Sen Lee, "Digital Image Enhancement and Noise Filtering by Use of Local Statistics," in IEEE Transactions on Pattern Analysis and Machine Intelligence, 1980, vol. 2, no. 2, pp. 165–168, doi: 10.1109/TPAMI.1980.4766994.

[22] A. Dostálová, M. Hollaus, M. Milenković, and W. Wagner, "Forest Area Derivation From Sentinel-1 Data," ISPRS Ann. Photogramm. Remote Sens. Spat. Inf. Sci., vol. III–7, no. February 2018, pp. 227–233, 2016, doi: 10.5194/isprsannals-iii-7-227-2016.

[23] M. Mahrooghy, J. Aanstoos, K. Hasan, S. Prasad, and N. H. Younan, "Effect of vegetation height and volume scattering on soil moisture classification using synthetic aperture radar (SAR) images," Proc. - Appl. Imag. Pattern Recognit. Work., 2011, doi: 10.1109/AIPR.2011.6176375.

[24] P. Ma, H. Zhang, C. Wang, and J. Chen, "Classification of forest vegetation species based on parameters of tomography," in 3rd International Asia-Pacific Conference on Synthetic Aperture Radar (APSAR) 2011, 2011, pp. 1–4.

[25] Y. Kim and J. J. Van Zyl, "A time-series approach to estimate soil moisture using polarimetric radar data," IEEE Trans. Geosci. Remote Sens., vol. 47, no. 8, pp. 2519–2527, 2009, doi: 10.1109/TGRS.2009.2014944.

[26] Y. Liu, W. Gong, X. Hu, and J. Gong, "Forest type identification with random forest using Sentinel-1A, Sentinel-2A, multi-temporal Landsat-8 and DEM data," Remote Sens., vol. 10, no. 6, pp. 1–25, 2018, doi: 10.3390/rs10060946.

[27] J. Kellndorfer, "Using SAR Data for Mapping Deforestation and Forest Degradation," in The SAR Handbook:Comprehensive Methodologies for Forest Monitoring and Biomass Estimation, A. I. Flores-Anderson, K. E. Herndon, R. B. Thapa, and E. Herrington, Eds. Huntsville: SERVIR Global Science, 2019, p. 16.

[28] B. a. M. Bouman, "Linking X-band radar backscattering and optical reflectance with crop growth models.," PhD Thesis. Wageningen Agric. Univ. Netherlands., 1991.

[29] A. P. Nicolau, A. Flores-Anderson, R. Griffin, K. Herndon, and F. J. Meyer, "Assessing SAR C-band data to effectively distinguish modified land uses in a heavily disturbed Amazon forest," Int. J. Appl. Earth Obs. Geoinf., vol. 94, no. July 2020, p. 102214, 2021, doi: 10.1016/j.jag.2020.102214.

[30] C. Dubois et al., "Characterization of land cover seasonality in sentinel-1 time series data," ISPRS Ann. Photogramm. Remote Sens. Spat. Inf. Sci., vol. 5, no. 3, pp. 97–104, 2020, doi: 10.5194/isprs-Annals-V-3-2020-97-2020.